VNU Journal of Science: Natural Sciences and Technology

Journal homepage: https://js.vnu.edu.vn/NST

Original Article

Synthesis of Chitosan Stabilized Silver Nanoparticles and Evaluation of the *in vitro* Antibacterial Activity Against *Xanthomonas oryzae* pv. *oryzae* Causing Blight Disease of Rice

Le Thi Hien[1,*], Nguyen Thi Phuong Hue[1], Le Trong Duc[1], Vu Thi Huyen[1], Le Thi Van[1], Hoang Thi Giang[2], Chu Duc Ha[1], Nguyen Thanh Ha[2], Nguyen Duy Phuong[2], Le Huy Ham[1,2]

[1]*VNU Univeristy of Engineering and Technology, 144 Xuan Thuy, Cau Giay, Hanoi, Vietnam*
[2]*Agricultural Genetics Institute, Vietnam Academy of Agricultural Sciences, Pham Van Dong, North Tu Liem, Hanoi, Vietnam*

Received 13 May 2021
Revised 30 July 2021; Accepted 02 August 2021

Abstract: Bacterial blight is one of the most devastating rice diseases that causes huge economic loss worldwide. The cause of rice blight is Gram negative bacteria *Xanthomonas oryzae* pv. *oryzae* (*X. oryzae* pv. *oryzae*). Since both silver nanoparticles and chitosan have antibacterial, antifungal and growth-stimulating effects, this work has focused on synthesizing chitosan stabilized silver nanoparticles (AgCSs) with small sizes and *in vitro* evaluating antibacterial activity against *X. oryzae* pv. *oryzae* bacteria. AgCSs were chemically synthesized by means of reducing silver nitrate with borohydride sodium in the presence of chitosan with optimization of the concentrations of the reactants. AgCSs were characterized by UV/vis absorption spectra, field emission scanning electronic microscopy (FESEM), ImageJ software, zeta potential measurement, Fourier-transform infrared spectroscopy (FTIR) and X-ray diffraction. AgCSs have spherical configuration and narrow size distributions with different average sizes from 15 nm to 25 nm depending on the initial concentration of silver nitrate. All AgCSs colloidal systems were stable and exhibited no tendency for coagulation after more than 5 months. For the first time, the *in vitro* antibacterial activity against bacterial blight *VXO_281* strain of chitosan stabilized silver nanoparticles was assessed. The disc diffusion method demonstrated that the smallest size silver nanoparticles (AgCS1) showed high antibacterial effect against the *X. oryzae* pv. *oryzae VXO_281* strain with a concentration of more than 5 µg/mL and the inhibition zone was dose-dependent. The minimum inhibitory concentration (MIC) and minimum bactericidal concentration (MBC) of AgCS1 against *X. oryzae* pv. *oryzae VXO_281* were 2.5 µg/mL and 20 µg/mL, respectively.

Keywords: Silver nanoparticles , chitosan, *Xanthomonas oryzae* pv. *oryzae*, blight disease.

* Corresponding author.
E-mail address: lehien@vnu.edu.vn

https://doi.org/10.25073/2588-1140/vnunst.5223

1. Introduction

Bacterial blight is one of the most devastating diseases of rice that causes severe yield loss in global cultivated areas [1]. It causes wilting of seedlings and yellowing, drying of leaves (Figure 1a). On young lesions, bacterial ooze can be observed early in the morning (Figure 1b). The cause of rice blight is *Xanthomonas oryzae pv. oryzae* (*X. oryzae* pv. *oryzae*). It is a gram-negative bacteria with a rod shape and is 0.55 ÷ 0.75 x 1.35 ÷ 2.17 μm (D × L) in size. The colonies of *X. oryzae* pv. *oryzae* are light yellow, circular, convex and smooth. *X. oryzae* pv. *oryzae* is favored by warm temperatures (25 to 30 °C), high humidity and environment with pH of 6.8 - 7.2 [2]. It is considerably challenging to figure out a sustainable solution to prevent the bacterial blight in rice plants.

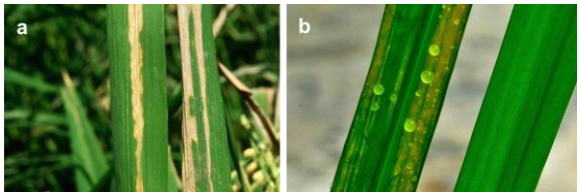

Figure 1. (a) Symptoms of blight disease in rice plants. (b) Bacterial ooze [1].

In recent years, great efforts have been made in order to apply the nanomaterials to control the *X. oryzae pv. oryzae* isolates, such as silver nanoparticles [3, 4], silicondioxide nanosphere loaded with silver nanoparticles [5], zinc nanoparticles and chitosan nanoparticles [6]. Initial results showed the positive inhibitory effect on the *X. oryzae pv. oryzae*, however, it requires more detailled investigations and field trials.

Silver nanoparticles were widely investigated in the last decades thanks to their antibacterial [7] and antifungal properties [8]. They have been used for many applications in cultivations not only as plant protection agents against bacterial [9] and fungal infections [10], but also as growth stimulants [11]. The aforementioned beneficial effects of silver nanoparticles depend on their morphology, size and composition (capping agents play a key role [12]).

Chitosan is an ecologically friendly, biodegradable material. It is a linear polysaccharide composed of randomly distributed β-(1→4)-linked N-acetyl-D-glucosamine and D-glucosamine that is produced by deacetylating the chitin shells of shrimp and other crustaceans with an alkaline solution. In crop production, chitosan is often used as a natural seed treatment, a plant growth enhancer [13] and a biopesticide substance that boosts the innate ability of plants to defend themselves against fungal infections [14, 15].

In the present work, we aimed to combine two above-mentioned materials to make use of their antibacterial and plant growth enhanced properties. The purpose of this work was to synthesize chitosan-stabilized silver nanoparticles with small sizes, narrow size distribution and to evaluate their antibacterial activity against *X. oryzae* pv. *oryzae* which is known for causing bacterial blight disease of rice.

2. Materials and Methods

2.1. Materials

Silver nitrate ($AgNO_3$, Fisher Chemical), sodium borohydride 98% ($NaBH_4$, Weng Jiang Reagent), chitosan (Bio Basic), L-glutamic acid ($C_5H_9NO_4$, Bio Basic), peptone-A (Weng Jiang Reagent), saccharose ($C_{12}H_{22}O_{11}$, Xilong Scientific). *X. oryzae* pv. *oryzae VXO_281* strain (*VXO_281*) was obtained from Molecular Pathology Department, Agricultural Genetics Institute, Vietnam Academy of Agricultural Sciences.

2.2. Methods

2.2.1. Synthesis of Silver Nanoparticles

AgCS1 was synthesized according to previouse works with some modifications [12, 16]. In brief, one volume of silver nitrate 3.8 mM ($AgNO_3$) solution and double volume of chitosan solution in acetic acid with various concentrations (0.2 - 1000 μg/mL) were added in to the Erlenmeyer flask, followed by slowly dripping one volume of sodium borohydride at 25 ^oC under magnetic stirring condition. The

reduction of silver nitrate solution by sodium borohydride solution was occurred based on the following reaction [17]:

$AgNO_3+NaBH_4=Ag+1/2H_2+1/2B_2H_6+NaNO_3$ (1)

The final concentration of silver was 0.95 mM (100 mg/l). In order to optimize the synthesis of AgCS1, the concentration of silver nitrate was fixed at 0.95 mM, concentrations of chitosan were varied from 0.1 to 500 µg/mL and concentrations of sodium borohydride were equal (1:1), double (1:2) and four times (1:4) the concentration of silver nitrate.

After the optimal concentrations of chitosan and $NaBH_4$ solutions for AgCS1 synthesis were determined, the synthesises of other chitosan stabilized silver nanoparticles (AgCS2, AgCS3, AgCS4, AgCS5) were conducted, using the optimal concentration ratios in the Table 1.

All solutions were preserved in dark at 25 ºC.

2.2.2. Characterization of Silver Nanoparticles

The absorption of AgCSs were measured by the Thermo Scientific NanoDrop 8000 spectrophotometer in the wavelength range of 300-600 nm.

The morphologies of AgCS1, AgCS3, AgCS5 were characterized by the Hitachi S4800 field-emission scanning electron microscope.

The size distributions of AgCSs were built by processing FESEM images with the Image software.

The synthesized AgCSs were separated by centrifugation at 12000 rpm for 15 minutes and analyzed by X-ray diffraction (XRD) on the XRD EQUINOX 5000 (Thermo Scientific, France) with X-ray source emitting Cu-Kα radiation (k = 1.5406 Å) and scans acquisition at 2θ range from 0 °C to 120 °C.

The zeta potential of AgCSs nano systems was measured via the Horiba SZ-100Z2 Zetasizer instrument at 25 °C.

Fourier transform infrared spectroscopy was performed by means of IR Prestige-21 Shimadzu Fourier transform infrared spectrophotometer at a grazing angle of 80 °C with the resolution 4 cm^{-1}.

2.2.3. Antibacterial Activity Test Against *X. oryzae* pv. *oryzae*

Disc diffusion test

The *X. oryzae* pv. *oryzae VXO_281* strain was grown for 48 hours in a 50 ml conical flask containing 15 mL of peptone sucrose nutrient broth at 28 °C on a rotatory shaker (200 rpm). An aliquot of 200 µL freshly grown culture (ca. 10^8 cfu/mL) was spread over nutrient agar petri plates. Wells with diameters of 6 mm were prepared with sterile equipment and filled with 15 µL of different concentrations of AgCS1 (5, 10, 20, 30, 50 and 100 µg/mL). The plates were incubated for 48 hours at 28 °C for observing the formation of inhibition zones (Δd) around the treated wells. Inhibition zone was calculated according to the formula:

$\Delta d = d_1 - d_0$, where d_1 is the diameter of the area without bacterial growth and d_0 is the diameter of the wells (6 mm).

The same volume of sterile deionized water was used as the control and 15 µl of different concentrations of chitosan (5, 10, 20, 30, 50 and 100 µg/mL) were utilized for comparison with AgCS1.

Experiments were carried out in triplicate and the average value of the inhibition zones was determined.

MIC and MBC determination

To determine the minimum inhibitory concentration (MIC), AgCS1 at various concentrations (0-30 µg/mL) were introduced into sterile falcons (volume of 50 ml) each containing 15 ml of peptone sucrose nutrient broth. The falcons were then inoculated with freshly prepared bacterial suspensions and an initial bacterial concentration of approximately 10^6 CFU/mL was maintained for all the experiments. The culture media were incubated for 24 hours (28 °C) in an orbital shaker at a high rotation speed of 200 rpm to avoid agglomeration of silver nanoparticles during incubation. An optical density at 600 nm of the culture media was measured by 7305 spectrophotometer (Jenway) after 24 hours of incubation. The MIC was determined as the minimum concentration of AgCS1 that made the OD600 of culture medium approximately zero after 24 hours of incubation.

The minimum bactericidal concentration (MBC) was determined using the culture for

evaluating MIC values. The samples that exhibit $OD_{600} \leq 0,04$ (had no or little bacterial growth) were selected and 50 µl from each flask was plated on a fresh peptone sucrose agar (PSA) medium and incubated for 48 hours at 28 °C. The lowest nanoparticle concentration causing bactericidal effect (the absence of colonies on an agar plate) was reported as MBC. Assessing MIC and MBC values was done in triplicate.

3. Results and Discussion

AgCSs of various sizes were synthesized using chitosan as capping and stabilizing agent and sodium borohydride as a reducing agent.

Figure 2. Scheme of AgCSs synthesis.

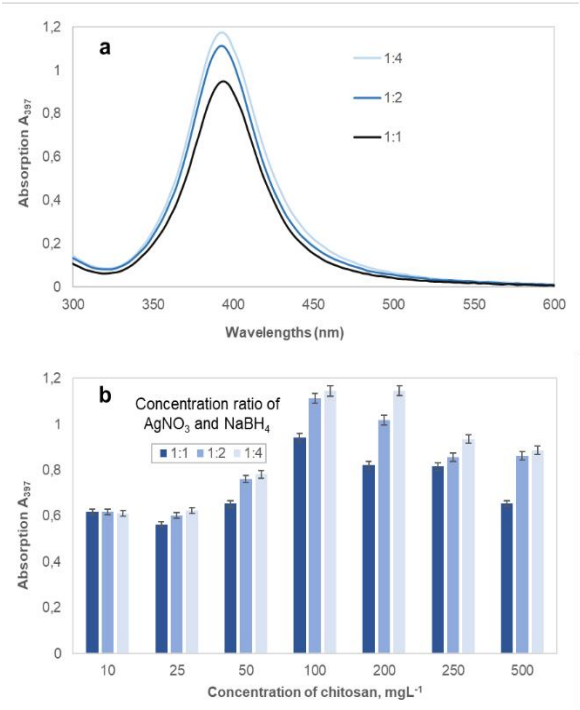

Figure 3. a. Absorption spectra of AgCS1 with various concentration ratios of $AgNO_3$ and $NaBH_4$ (1:1, 1:2 and 1:4). b. Absorption at 397 nm of AgCS1 with different concentrations of chitosan and $NaBH_4$.

3.1. Optimizing of Synthesis

The formation of AgCSs was investigated by their UV/vis absorption spectra and the maximal absorption at the wavelength of 397 nm (A_{397}). It was shown that AgCSs were formed if the chitosan concentration was higher than 1 µg/mL ($A_{397}>0$). A_{397} reached the maximal value at the chitosan concentration of 100 µg/mL (Figure 3b). In addition, the A_{397} values of AgCS1 were increasing when the concentration of $NaBH_4$ was equal (1:1), double (1:2) or four times (1:4) the concentration of $AgNO_3$ (Figure 3a). However, the A_{397} values of AgCS1 with 1:2 and 1:4 concentration were approximately the same. Therefore, the optimal concentrations for synthesis of AgCS1 are 0.95 mM silver nitrate, 100 µg/mL chitosan and 1.9 mM $NaBH_4$ (Table 1).

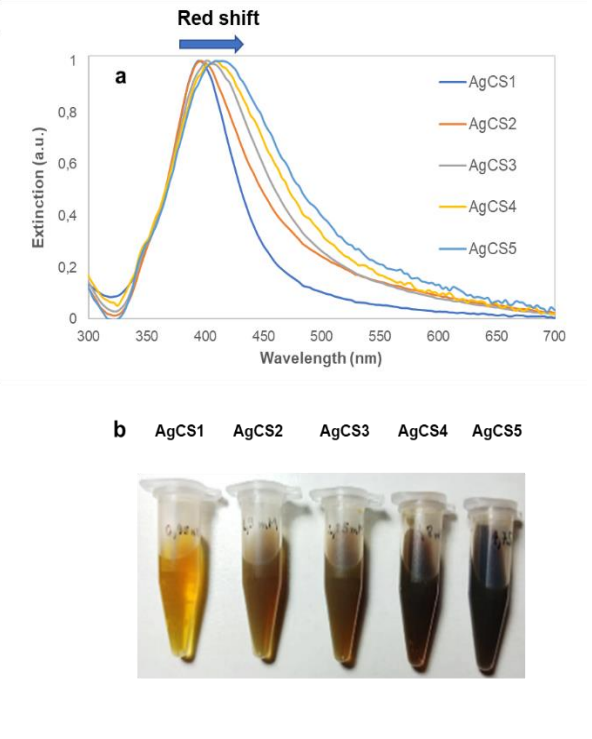

Figure 4. Normalized UV/vis absorption spectra (a) and distinctive colors (b) of AgCSs with different sizes.

3.2. Characterization of Chitosan Silver Nano Particles

As presented in Figure. 4a, AgCSs have sharp UV/vis absorption peaks at 397, 403, 409, 415, 418 nm wavelengths for AgCS1, AgCS2, AgCS3, AgCS4 and AgCS5, respectively. The maximal absorption wavelengths of AgCSs were red-shifted with increasing in their sizes, which is consistent with previous reports [7]. The full width at half maximum (FWHM) of the peaks extended from 36 to 114 nm for AgCS1 to AgCS5 indicated the rising polydispersity of nanoparticle colloids (Table 1). Higher concentrations of silver nitrate, chitosan and borohydride sodium were crucial for synthesizing silver nanoparticles with larger sizes. The distinctive colors of AgCSs with different sizes and concentrations are demonstrated in Figure 4b.

The morphology of AgCSs was observed using FESEM. As shown in Figure 5a, the majority of the chitosan silver nanoparticles are spherical. The particle size distributions of AgCSs were presented on the Figure 5b, which indicated the average size of 15, 20 and 25 nm for AgCS1, AgCS3, AgCS5, respectively.

The absolute zeta potential values of nano systems can be utilized as a stability indicator of the colloidal systems: the higher zeta potential is, the more stable the colloidal system is. Since chitosan is a polymer with amino functional groups, the chitosan based silver nanoparticle systems get positive zeta potential. The absolute zeta potential values of AgCS nano systems were beyond the limits of the (−30, +30) mV region (Table 1), which indicated that all of them could be considered as stable systems [12]. In addition, zeta potential values of AgCS nano systems slightly increased from AgCS5 to AgCS1 systems, which showed the rise of stability in this order.

As shown in Figure 6a, the X-ray diffractogram of the AgCSs has the characteristic peaks corresponding to the inter-planar distances of the crystalline silver. Four Bragg reflections at 2θ of AgCS1 (38.28, 44.48, 64.44, 77.25) and AgCS5 (38.23, 44.25, 64.11, 76.95) were corresponding to the (111), (200), (220) and (311) plans, respectively. This result confirmed that the AgCSs were formed of crystalline nanostructures and possessed a face-centered cubic (fcc) lattice [18].

Calculating the size of the crystalline AgCS1 and AgCS5 using Scherrer equation with the FWHM of the most intense reflection (111) peak from the XRD data revealed their sizes of 16.0 nm and 23.1 nm, respectively. These results are consistent with the results of the FESEM analysis.

Figure 6b shows the FTIR spectra of chitosan of AgCS1 and AgCS5. Two peaks at 1600 and 1655 cm^{-1} due to bending vibration of NH_2 group and stretching vibration of C = O in $NHCOCH_3$ in pure chitosan converted into one peak 1640 or 1637 cm^{-1} in the AgCS1 and AgCS5, respectively. This conversion indicated the interaction between silver and amino groups of chitosan in nanoparticles. In addition, the fingerprint region of chitosan from 1020 to 1450 cm^{-1} [19], including the asymmetric stretching vibration of C-O-C (glycosidic linkage) (1083 cm^{-1}), stretching vibration ofC-O in secondary alcohol (1030 cm^{-1}), disappeared in both AgCS1 and AgCS5. Furthermore, the bending vibration of CH_2 group in CH_2OH (1423 cm^{-1}) and in-plane scissoring of CH_3 in $NHCOCH_3$ (1381 cm^{-1}) dramatically decreased in both AgCS1 and AgCS5. The significant changes in FTIR spectra of AgCSs in comparison with FTIR spectra of chitosan were likely to be caused by the interaction between silver and different functional groups of chitosan including amino groups, glycosidic linkages, secondary OH and $NHCOCH_3$.

All AgCSs stored at 25 °C without direct sunlight exhibited no tendency for coagulation after more than 5 months. However, the maximal UV/vis absorption decreased gradually at most approximately 7% with constant λ_{max}.

Table 1. Concentration of reactants and some characteristics of AgCSs

Samples	C_{AgNO3} (mM)	$C_{chitosan}$ (µg/mL)	C_{NaBH4} (mM)	λ_{max} (nm)	$A(\lambda_{max})/A_0^*$	FWHM	Particle size (nm)	Zeta potential (mV)
AgCS1	0.95	100	1.9	397	1	36	15	47.7±1.6
AgCS2	1.9	200	3.8	403	1.2	81	ND	42.9±0.7
AgCS3	2.85	300	5.7	409	2.1	93	20	40.2±1.1
AgCS4	3.8	400	7.6	415	2.7	105	ND	38.7±0.9
AgCS5	4.95	500	9.9	418	3.0	114	25	35.7±0.7

* A_0 is maxmal absorption of AgCS1, A(λ max) is maxmal absorption of other AgCSs.
ND represents not determined in this work.

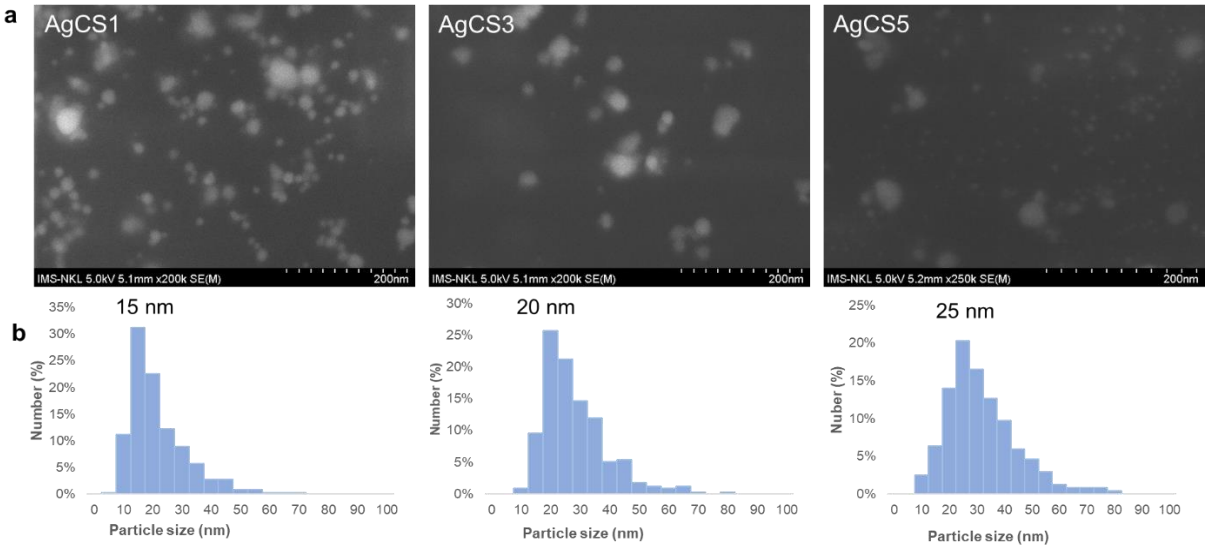

Figure 5. FESEM (a) and particle-size distributions (b) of AgCS1, AgCS3, AgCS5.

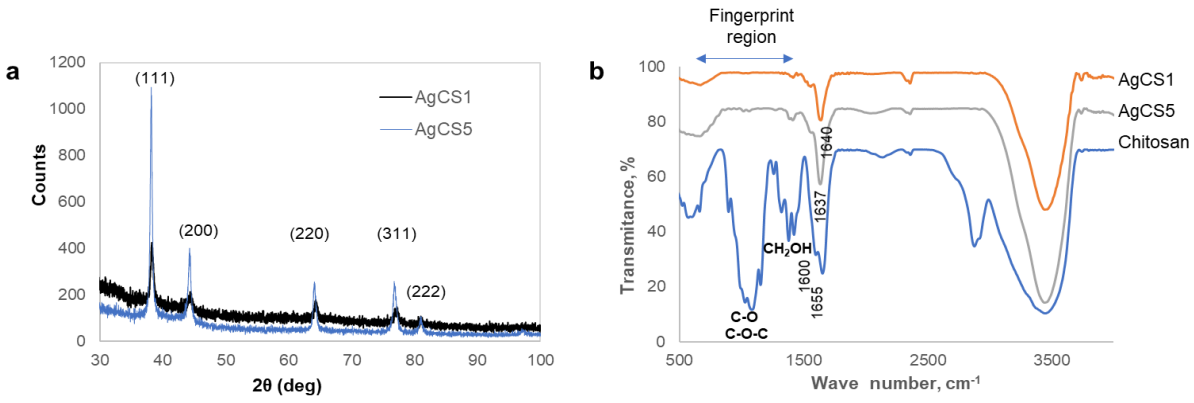

Figure 6 a. XRD pattern of the AgCS1 and AgCS5. b. FTIR spectra of chitosan of theAgCS1 and AgCS5.

3.3. Evaluation of in Vitro Antibacterial Activity Against X. oryzae pv. oryzae

Antibacterial potential of the smallest size (15 nm) AgCS1 against *VXO_281* strain was assessed by the disc diffusion test. As demonstrated in Figure 7a, an inhibition zone appeared when the concentration of AgCS1 was greater than or equal to 5 µg/mL and was increased in a dose-dependent manner. Meanwhile, the control discs with deionized water and chitosan with concentrations ranging from 5 - 50 µg/mL had no inhibition zone. When the concentration of chitosan reached the value of 100 µg/mL, an inhibition zone of only 4 mm was observed (Figure 7b). These results indicated that the silver nanoparticles were effective antibacterial components of the chitosan-stabilized silver nanoparticles. In addition, inhibitory effect in bacterial growth was highly related to the concentrations of AgCS1. Since the used concentration of $NaBH_4$ was twice concentration of $AgNO_3$, it was supposed that most silver ions had been reduced to form AgCS1. Therefore, AgCS1 probably contributed to the main antibacterial activity of the system.

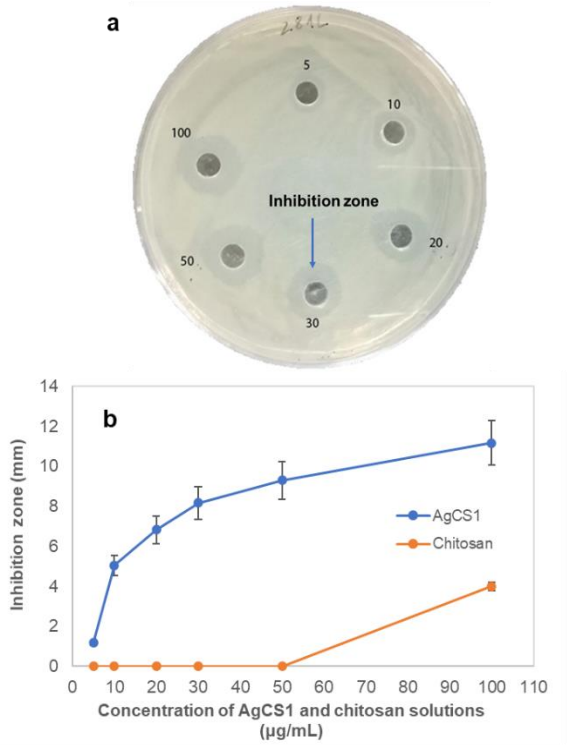

Figure 7 a. Zone of inhibition for AgCS1 with different concentrations of 5 to 100 µg/mL against *VXO_281* strain on peptone sucrose agar petri dish. An arrow indicates inhibition zone of AgCS1 loading in well.
b. The graph of inhibition zones vs. concentration of AgCS1 and chitosan solutions as control.

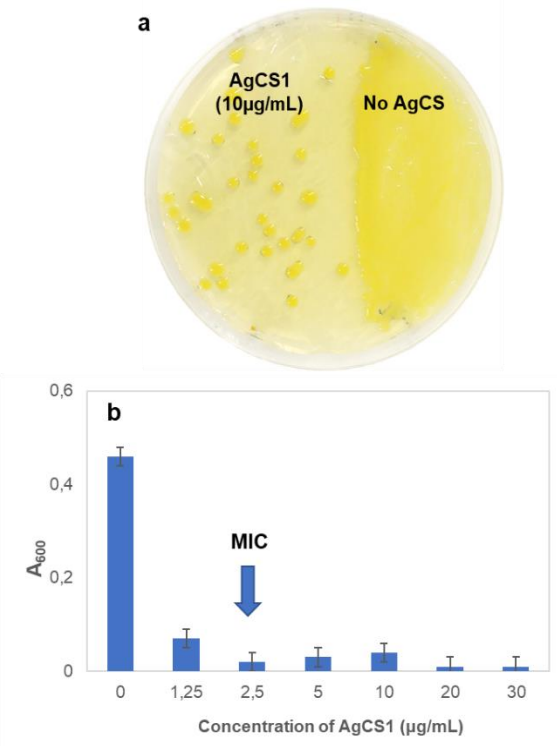

Figure 8 a. The graph of optical density at 600 nm of the bacterial medium with AgCS1 concentration of 0-30 µg/mL after 24 hours of incubation.
b. The growth of *VXO_281* strain colonies with no AgCS1 and with AgCS1 (10 µg/mL).

However, how silver ions are released from AgCSs and what is the antibacterial mechanism of AgCSs against *X. oryzae* pv. *oryzae* are not clear, which is recommended for future research.

In comparison with the biosynthesized silver nanoparticles (12 nm in size) which demonstrated inhibitory dose against *X. oryzae* pv. *oryzae* strains in the range of 20-50 µg/mL [3], AgCS1 showed higher significant antibacterial activity. This is demonstrated by the inhibition zone appearing when the concentration of AgCS1 was greater than or equal to 5 µg/mL.

Minimal inhibitory concentration (MIC) and minimum bactericidal concentration (MBC) testing against *VXO_281* strain were performed to further assess the antibacterial activity of the AgCS1. As demonstrated in Figure 8a, an optical density at 600 nm of the culture medium reached an insignificantly small value when the concentration of the AgCS1 was 2,5 µg/mL, therefore the MIC is 2,5 µg/mL. The absence of colonies on agar plate was observed when the concentrations of AgCS1 were 20 and 30 µg/mL, while at the concentration of 10 µg/mL, there were ca. 40 colonies, as shown in Figure 8b. Hence the MBC of AgCS1 against *VXO_281* strain was 20 µg/mL.

It was not rational to compare MIC and MBC values of antibacterial agents against *X. oryzae* pv. *oryzae* in different studies, because these values depend on various factors, such as bacterial strains with different virulence, initial bacterial concentration and experiment conditions. However, in comparison with other studies using nearly the same initial concentration of *X. oryzae* pv. *oryzae* (10^6 cfu/ml), the AgCS1 in this study showed lower MIC (2.5 µg/mL). Both the biosynthesized silver nanoparticles using the endophytic bacteria *Bacillus siamensis* with the size of 25-50 nm AgNPs [20] and *Bacillus cereus* SZT1 with the size ranging from 18 to 39 nm [21] depicted MIC values of 20 µg/mL for *X. oryzae* pv. *oryzae* strains. This means that AgCS1 in this study has a better antibacterial activity against *X. oryzae* pv. *oryzae.*

4. Conclusion

This study highlights the optimization of synthesis of chitosan-stabilized silver nanoparticles. It is the first time that chitosan-stabilized silver nanoparticles were assessed the *in vitro* antibacterial activity against bacterial blight *VXO_281* strain. This study showed that the chitosan-stabilized silver nanoparticles have a great potential to suppress *X. oryzae* pv. *oryzae* infections in rice.

Acknowledgements

This work was finacially supported by the VNU University of Engineering and Technology under project CN 19.01.

References

[1] International Rice Research Institute, https://www.irri.org/disease-and-pest-resistant-rice/, http://www.knowledgebank.irri.org/decision-tools/rice-doctor/rice-doctor-fact-sheets/item/bacterial-blight/, 2020 (accessed on: February 10th, 2020).

[2] M. Sullivan, E. Daniells, C. Southwick, CPHST Pest Datasheet for *Xanthomonas oryzae pv. oryzae*, USDA-APHIS-PPQ-CPHST, 2016.

[3] S. Mishra, X. Yang, S. Ray, L. F. Fraceto, H. B. Singh, Antibacterial and Biofilm Inhibition Activity of Biofabricated Silver Nanoparticles Against *Xanthomonas oryzae pv. oryzae* Causing Blight Disease of Rice Instigates Disease Suppression, World Journal of Microbiology and Biotechnology, Vol. 36, 2020, pp. 55-64.

[4] H. Shang, Z. Zhou, X. Wu, X. Li, Y. Xu, Sunlight-induced Synthesis of Non-target Biosafety Silver Nanoparticles for the Control of Rice Bacterial Diseases, Nanomaterials, 2007.

[5] J. Cui, Y. Liang, D. Yang, Y. Liu, Facile Fabrication of Rice Husk Based Silicon Dioxide Nanospheres Loaded with Silver Nanoparticles as a Rice Antibacterial Agent, Scientific Reports, Vol. 6, 2016, pp. 21423-21432.

[6] Y. Abdallah, M. Liu, S. O. Ogunyemi, T. Ahmed, H. Fouad, A. Abdelazez, C. Yan, Y. Yang, J. Chen, B. Li, Bioinspired Green Synthesis of Chitosan and Zinc Oxide Nanoparticles with Strong Antibacterial Activity Against Rice Pathogen *Xanthomonas*

oryzae pv. oryzae, Molecules, Vol. 25, 2020, pp. 4795-4812.

[7] S. Agnihotri, S. Mukherji, S. Mukherji, Size-controlled Silver Nanoparticles Synthesized Over the Range 5-100 nm Using the Same Protocol and Their Antibacterial Efficacy, Royal Society of Chemistry Advances, Vol. 4, 2014, pp. 3974-3983.

[8] Y. A. Krutyakov, A. A. Kudrinskiy, P. M. Zherebin, A. D. Yapryntsev, M. A. Pobecdinskaya, S. N. Elansky, A. N. Denisov, D. M. Mikhaylov G. L. Lisichkin, Tallow Amphopolycarboxyglycinate-stabilized Silver Nanoparticles: New Frontiers in Development of Plant Protection Products with a Broad Spectrum of Action Against Phytopathogens, Materials Research Express, Vol. 3, 2016, pp. 075403-07541.

[9] M. Kumari, P. Pandey, A. Bhattacharya, A. Mishra, C. S. Nautiyal, Protective Role of Biosynthesized Silver Nanoparticles Against Early Blight Disease in *Solanum lycopersicum*, Plant Physiology and Biochemistry, Vol. 121, 2017, pp. 216-225.

[10] M. S. Nejad, G. H. Shahidi Bonjar, M. Khatami, A. Amini, S. Aghighi, In Vitro and in Vivo Antifungal Properties of Silver Nanoparticles Against Rhizoctonia Solani, a Common Agent of Rice Sheath Blight Disease, IET Nanobiotechnol, Vol. 11, 2017, pp. 236-240.

[11] O. V. Zakharova, A. A. Gusev, P. M. Zherebin, E. V. Skripnikova, M. K. Skripnikova, V. E. Ryzhikh, G. V. Lisichkin, O. A. Shapoval, M. E. Bukovskii, Y. A. Krutyakov, SodiumTallow Amphopolycarboxyglycinate-stabilized Silver Nanoparticles Suppress Early and Late Blight of Solanum Lycopersicum and Stimulate the Growth of Tomato Plants, BioNanoScience, 2017.

[12] Y. A. Krutyakov, A. A. Kudrinskiy, P. M. Zherebin, G. V. Lisichkin, Correlation between the Rate of Silver Nanoparticle Oxidation and Their Biological Activity: the Role of the Capping Agent, Journal of Nanoparticle Research, Vol. 21, 2019, pp. 69-85.

[13] M. M. A. Mondal, M. A. Malek, A. B. Puteh, M. R. Ismail, M. Ashrafuzaman, L. Naher, Effect of Foliar Application of Chitosan on Growth and Yield in Okra, Australian Journal of Crop Science, Vol. 6, 2012, pp. 918-921.

[14] M. A. Trzcińska, A. Bogusiewicz, M. Szkop, S. Drozdowski, Effect of Chitosan on Disease Control and Growth of Scots pine (*Pinus sylvestris L.*) in a Forest Nursery, Forests, Vol. 6, 2015, pp. 3165-3176.

[15] M. Sathiyabama, G. Akila, R. C. Einstein, Chitosan-induced Defence Responses in Tomato Plants Against Early Blight Disease Caused by *Alternaria solani* (Ellis and Martin) Sorauer, Archives Of Phytopathology And Plant Protection, Vol. 47, 2014, pp. 1777-1787.

[16] C. Pansara, R. Mishra, T. Mehta, A. Parikh, S. Garg, Formulation of Chitosan Stabilized Silver Nanoparticle-containing Wound Healing Film: *In Vitro* and *in Vivo* Characterization, Journal of Pharmaceutical Sciences, Vol. 109, 2020, pp. 2196-2205.

[17] L. Pourzahedi, M. Eckelman, Comparative Life Cycle Assessment of Silver Nanoparticle Synthesis Routes, Environmental Science Nano, Vol. 5, 2015, pp. 361-369.

[18] F. Laghrib, N. Ajermoun, M. Bakasse, S. Lahrich, M. A. El Mhammedi, Synthesis of Silver Nanoparticles Assisted by Chitosan and Its Application to Catalyze the Reduction of 4-nitroaniline, International Journal of Biological Macromolecules, Vol. 135, 2019, pp. 752-759.

[19] S. Bhardwaj, N. Bhardwaj, Y. Negi. Effect of Degree of Deacetylation of Chitosan on Its Performance as Surface Application Chemical for Paper-based Packaging, Cellulose, Vol. 27, 2020, pp. 5337-5352.

[20] E. Ibrahim, H. Fouad, M. Zhang, Y. Zhang, W. Qiu, C. Yan, B. Li, J. Moc, J. Chen, Biosynthesis of Silver Nanoparticles Using Endophytic Bacteria and Their Role in Inhibition of Rice Pathogenic Bacteria and Plant Growth Promotion, Royal Society of Chemistry Advances, Vol. 9, 2019, pp. 29293-29299.

[21] T. Ahmed, M. Shahid, M. Noman, M. Niazi, F. Mahmood, I. Manzoor, Y. Zhang, B. Li, Y. Yang, C. Yan, J. Chen, Silver Nanoparticles Synthesized by Using Bacillus Cereus SZT1 Ameliorated the Damage of Bacterial Leaf Blight Pathogen in Rice, Pathogens, Vol. 9, 2020, pp. 160-176.